International Journal of Radiation Oncology biology • physics

www.redjournal.org

Physics Contribution

MR-OPERA: A Multicenter/Multivendor Validation of Magnetic Resonance Imaging—Only Prostate Treatment Planning Using Synthetic Computed Tomography Images

Emilia Persson, MSc,[*,†] Christian Gustafsson, MSc,[*,†] Fredrik Nordström, PhD,[‡] Maja Sohlin, MD, PhD,[‡] Adalsteinn Gunnlaugsson, MD, PhD,[*] Karin Petruson, MD, PhD,[§] Niina Rintelä, MSc,[‖] Kristoffer Hed, BSc,[‖] Lennart Blomqvist, MD, PhD,[¶,#,] Björn Zackrisson, MD, PhD,[¶] Tufve Nyholm, PhD,[¶,††] Lars E. Olsson, PhD,[†] Carl Siversson, PhD,[‡‡] and Joakim Jonsson, PhD[¶]**

Department of Hematology, Oncology, and Radiation Physics, Skåne University Hospital, Lund; [†]Department of Medical Physics, Lund University, Malmö; Departments of [‡]Medical Physics and Biomedical Engineering, and [§]Oncology, Sahlgrenska University Hospital, Gothenburg; [‖]Medical Radiation Physics and Nuclear Medicine, and **Department of Diagnostic Radiology, Karolinska University Hospital, Stockholm; [¶]Department of Radiation Sciences, Umeå University, Umeå; [#]Department of Molecular Medicine and Surgery, Karolinska Institutet, Stockholm; [††]Department of Immunology, Genetics, and Pathology, Uppsala University, Uppsala; and [‡‡]Spectronic Medical AB, Helsingborg, Sweden

Received Nov 1, 2016, and in revised form May 12, 2017. Accepted for publication Jun 7, 2017.

Summary

This study aimed to validate a commercially available software for MR to synthetic computed tomography (CT) conversion for use in an MRI-only prostate external radiation therapy workflow.

Purpose: To validate the dosimetric accuracy and clinical robustness of a commercially available software for magnetic resonance (MR) to synthetic computed tomography (sCT) conversion, in an MR imaging—only workflow for 170 prostate cancer patients.

Methods and Materials: The 4 participating centers had MriPlanner (Spectronic Medical), an atlas-based sCT generation software, installed as a cloud-based service. A T2-weighted MR sequence, covering the body contour, was added to the clinical protocol. The MR images were sent from the MR scanner workstation to the

Reprint requests to: Emilia Persson, MSc, Department of Hematology, Oncology, and Radiation Physics, Skåne University Hospital, Klinikgatan 5, 22185 Lund, Sweden. Tel: (+46) (0) 72-509-00-75; E-mail: Emilia.Persson@skane.se

Funding: This work was partially funded by Vinnova, Sweden's innovation agency, through the national project Gentle Radiotherapy with grant number 2016-03847, 'Allmänna sjukhusets i Malmö Stiftelse för bekämpande av cancer', The Swedish testbed for innovative radiation therapy and Skånes Universitetssjukhus stiftelser.

Conflict of interest: F.N. and C.S. are employed by Spectronic Medical.

Acknowledgment—The authors thank the clinical staff at the centers for their excellent help throughout the study.

Int J Radiation Oncol Biol Phys, Vol. 99, No. 3, pp. 692—700, 2017

http://dx.doi.org/10.1016/j.ijrobp.2017.06.006

A multicenter study design was used to compare CT-based treatment plans with recalculated synthetic CT plans for 170 prostate cancer patients. The software was found to be robust for a variety of field strengths, vendors, and treatment techniques.

MriPlanner platform. The sCT was automatically returned to the treatment planning system. Four MR scanners and 2 magnetic field strengths were included in the study. For each patient, a CT-treatment plan was created and approved according to clinical practice. The sCT was rigidly registered to the CT, and the clinical treatment plan was recalculated on the sCT. The dose distributions from the CT plan and the sCT plan were compared according to a set of dose-volume histogram parameters and gamma evaluation. Treatment techniques included volumetric modulated arc therapy, intensity modulated radiation therapy, and conventional treatment using 2 treatment planning systems and different dose calculation algorithms.

Results: The overall (multicenter/multivendor) mean dose differences between sCT and CT dose distributions were below 0.3% for all evaluated organs and targets. Gamma evaluation showed a mean pass rate of 99.12% (0.63%, 1 SD) in the complete body volume and 99.97% (0.13%, 1 SD) in the planning target volume using a 2%/2-mm global gamma criteria.

Conclusions: Results of the study show that the sCT conversion method can be used clinically, with minimal differences between sCT and CT dose distributions for target and relevant organs at risk. The small differences seen are consistent between centers, indicating that an MR imaging−only workflow using MriPlanner is robust for a variety of field strengths, vendors, and treatment techniques.

Introduction

The limited soft tissue contrast of computed tomography (CT) images makes definition of the target and organs at risk (OARs) difficult for radiation therapy treatment planning. This has led to the widespread introduction of magnetic resonance imaging (MRI) into radiation therapy clinics during recent years (1). Magnetic resonance imaging exhibits excellent soft tissue contrast and has been shown to increase accuracy in target definitions for several tumor sites, as well as to add value to the delineation of OARs (2-6). Although MR images have an important role in the delineation process, CT imaging has retained its position as the imaging modality of choice for the treatment planning process (dose calculation and generation of images for patient positioning). This is mainly attributed to the high geometric accuracy of CT and its unique relationship to the attenuation of the imaged tissue, which is needed for inhomogeneity-corrected dose calculations. To accomplish this multimodal approach of treatment preparation, image registration has been widely used to transfer MR-based treatment volumes to the CT images used for treatment planning.

There are, however, several disadvantages with this workflow. The cost of using multiple imaging modalities in the preparation steps of radiation therapy is not insignificant, and the geometric uncertainty associated with the co-registration of MR and CT images acquired at different time points and at different imaging devices may be significant. In absolute numbers the uncertainties in CT-MR registration has been estimated to be 2 mm (1 SD) (7). Systematic registration errors will propagate through the treatment planning process and cause a systematic error that will persist throughout the entire treatment. In contrast to random errors, such as those introduced by day-to-day positioning, the systematic errors are more serious and could lead to a displacement of the dose distribution (8). This has led several groups to investigate the possibilities of using MRI only for both delineations and treatment planning, under the assumption that the uncertainty in the identification of the markers based on MR data will be smaller than the uncertainty in the co-registration between CT and MR.

To allow dose calculations based on MRI, methods have been developed to convert MR images to images similar to CT, often denoted as synthetic CT (sCT) images. Several methods have been proposed: (*1*) direct conversion of pixel values using specialized sequences, such as ultra-short echo time imaging in combination with other sequences (9-11); (*2*) population atlas techniques, which use deformable image registration to warp a label image to an MR image (12-15); or (*3*) a voxel-based affine registration approach (16). Further, manual and semi-manual segmentation techniques to divide an MR image into tissue classes that are assigned electron densities exist (17-20). All of these techniques have shown promising results, with point or mean dose deviations to the target in the vicinity of 1%. These studies have often been limited in terms of size of the patient cohorts and are mostly single-center studies, with a single scanner and field strength, using in-house-developed software. This has limited the widespread adoption of MRI-only treatment planning.

In this MR-Only Prostate External RAdiotherapy (MR-OPERA) study, the aim was to verify the dosimetric accuracy and robustness to clinical input data of a commercially available software for MR to sCT conversion of the male pelvis. The

atlas-based generation algorithm used in the software has previously been described (21). The study included 170 patients from 4 different university hospitals in Sweden, using different MR vendors and field strengths.

Methods and Materials

Patients

From October 2015 to June 2016, a total of 170 consecutive patients were included in a non-interventional, prospective, multicenter study, approved by the Umeå Regional ethics review board. Inclusion criteria were patients referred to MR and CT imaging before prostate radiation therapy. No height, weight, or age restrictions were imposed; however, patients with large surgical implants such as hip prosthesis were not eligible. Study participation did not affect the prescribed treatment, because the doses were recalculated to simulate MRI-only treatment.

Imaging

The conversion software used in the study required a T2-weighted MR image with large field of view (FOV), covering the entire patient contour, with sufficient coverage for treatment planning in the cranio-caudal direction. Further, the sequence was required to be corrected for geometric distortions and acquired with sufficient bandwidth to limit the impact of these. Such sequence was added to the standard protocol consisting of target and marker localization sequences (scan time 30-45 minutes). The study sequence was limited to approximately 5 minutes. All centers imaged the patients in treatment position on both CT and MR, using a flat tabletop and immobilization with ankle and knee support. Magnetic resonance and CT imaging parameters are specified in Tables 1 and 2. The RF (radiofrequency) coils, 18-channel body 18 long (used for the 2 Siemens scanners) and 16-channel GEM Anterior Array (used for the 2 GE scanners), were centered over the symphysis on a stiff coil bridge. Quality assurance of the MR scanners was performed according to local practice at each center.

sCT generation and treatment planning

The algorithm used in the conversion software MriPlanner (Spectronic Medical, Helsingborg, Sweden) has previously been described (21). The algorithm is based on an automated atlas-based conversion method that requires T2-weighted MR images for sCT generation. Since the previous publication the software has been updated with a new training data set, acquired at a single center. In practice the software integrates into the clinical workflow by configuring a Digital Imaging in Communications and Medicine (DICOM) node within the hospital, which receives and anonymizes patient data and generates a key. The anonymized patient data is then automatically uploaded to a cloud-based conversion service, which generates the sCT and returns it to the DICOM node. The patient information is restored using the previously generated key, and the sCT is automatically returned to the radiation therapy department for treatment planning.

One modification of the MriPlanner workflow was needed for this study: the CT was also uploaded to the cloud service so that the generated sCT could be rigidly registered according to bony anatomy to the CT before replanning. The sCT was returned with the same resolution as the CT. This additional step was needed to account for patient rotations between MR and CT. A simple treatment planning isocenter translation would result in a rotated dose distribution, which would limit the possibility of accurate comparisons.

A CT-based treatment plan was created according to clinical practice at each clinic (for technical details see Table 3). The CT plan was transferred to the rigidly registered sCT, and the dose was recalculated, resulting in 2 plans with identical beam setup. Target volumes and OARs were transferred from the CT to the sCT, whereas separate external contours were created for the CT and sCT images.

Evaluation

The dose-volume histogram (DVH) evaluation was carried out in CERR (version 4.6), a computational environment for radiation therapy research (22), between the original CT plan and the recalculated sCT plan, using the resulting dose matrices and CT structures. The protocol from the conventional arm in the Swedish multicenter phase 3 study of hypo-fractionated radiation therapy of intermediate-risk localized prostate cancer (23) was used as a reference for the dose-volume criteria to be evaluated. Gamma evaluation (24) was carried out using Medical Interactive Creative Environment, version 0.3.0.209 (available at www.gentleradiotherapy.se) (25) within the complete volumes,

Table 1 Imaging devices used at all centers

Center (no. of patients)	CT scanner	MR scanner and field strength
Center 1 (68)	Siemens Somatom Definition AS+	GE Discovery, 750w 3.0T
Center 2 (54)	Philips Brilliance Big Bore	GE Signa, PET/MR 3.0T
Center 3 (42)	Toshiba Aquilion LB	Siemens Aera 1.5T
Center 4 (6)	Siemens Somatom Definition AS+ or GE LightSpeed RT16	Siemens Skyra 3.0T

Abbreviations: MR = magnetic resonance; PET = positron emission tomography.

Table 2 Scan protocol parameters for the T2-weighted MR used for sCT generation

Parameter	MR scan	CT
Slice thickness (mm)	2.5-3.0	2.5-3.0
kV		120
Resolution x/y plane (mm)		1/1
Resolution x/y plane (recon.) (mm)	0.44-0.88/0.44-0.88	
Slice gap (mm)	0	
Distortion correction	On	
Bandwidth 3T (Hz/pixel)	244-390	
Bandwidth 1.5T (Hz/pixel)	215	
FOV (mm)	448	
No. of slices	88-100	
Time to echo (ms)	96-98	
Time to repetition (ms)	11,930-15,000	
Flip angle (°)	130-160	
Slice acquisition	2-Dimensional	
Postprocessing	Homogenization	
Sequence type	Spin echo	

Abbreviations: CT = computed tomography; FOV = field of view; kV = kilovoltage; MR = magnetic resonance; sCT = synthetic CT.

with a dose cutoff at 15% and within the planning target volume using global gamma criteria of 3%/3 mm, 2%/2 mm, and 1%/1 mm. The gamma calculations within MICE are implemented according to the method described by Wendling et al (26).

Two 1-sided tests of equivalence for paired samples (TOST-P) (27) were performed with an equivalence interval of (−0.5%, 0.5%) for all evaluated DVH criteria at a 95% confidence level. Dose criteria were evaluated as percentage of the prescribed dose and the volume criteria as absolute volume difference in percentage units. Equivalence testing is used to prove equality.

Differences in the external contour can arise owing to repositioning between CT and MR, which affects the sCT dose calculation and comparison. To investigate how differences in the external contours between the CT and sCT affected the dose comparison, a subset of patients (n = 28, prescribed 78 Gy to the prostate, included at center 1) were further evaluated using an sCT that was corrected to have the same external contour as the CT. After the rigid registration of the sCT and CT, the CT external contour was used to create a new sCT external contour. Air inside of the new external contour was replaced with water, and tissue outside the new external contour was removed and replaced with air.

Table 3 Summary of the treatment planning techniques used for all centers and patient-specific aspects for the 145 evaluated patients

Parameter	No. of patients
Target	
Prostate	76
Prostate and vesicles	52
Prostate, vesicles, and iliac lymph nodes	17
Prescribed dose (Gy) − fractionation (Gy/fraction × fractions)	
78 − 2 × 39	78
77 − 2.2 × 35	3
74 − 2 × 25 + 3 × 8	2
72.5 − 2.5 × 29	3
66 − 3 × 22	18
63 − 3 × 21	3
50 − 2 × 25	25
45 − 3 × 15	5
28 − 2 × 14, boost plan	8
Treatment technique	
IMRT	20
VMAT	107
Conventional, 3-field	18
Treatment planning system	
Varian Eclipse	100
Elekta Oncentra MasterPlan	45
Calculation model	
AAA	100
PB	45

Abbreviations: AAA = anisotropic analytical algorithm; IMRT = intensity modulated radiation therapy; PB = pencil beam; VMAT = volumetric modulated arc therapy.

Results

All patients who were uploaded to MriPlanner had successfully generated sCTs, including patients who were subsequently excluded owing to deviations from the study protocol (see below). The exclusions were due to operator fault or incorrect inclusion of study participants. The software was integrated into the current clinical workflows without modifications or any additional procedures. The mean (range) body mass index of the study population was 26.9 (18.0-37.7) kg/m^2, and median (range) age was 72 (56-87) years.

After inclusion a total of 25 patients had to be excluded owing to 3-dimensional distortion correction inadvertently being turned off (n = 12), the entire body contour was not included inside the FOV (n = 4), limited FOV in slice direction due to operator fault (n = 2), inclusion despite hip implants noted after MR imaging (n = 2), extreme difference in rectum filling between MR and CT (n = 1), patient included having been injected with an anatomy-distorting gel between prostate and rectum (n = 1), extremely poor image quality of MR image (n = 1), and patients imaged without coil holder (n = 2), leaving a total of 145 patients available for evaluation. Eight patients with nodal involvement had an insufficient FOV in the slice direction to cover the complete target. Their boost plans, covering the prostate, were calculated. Figure 1 displays the height and weight distribution of the study population.

The mean dose deviations between sCT and CT were found to be very small, below 0.3% for all evaluated organs and targets; for a complete DVH comparison, see Table 4. With an equivalence interval of (−0.5%, 0.5%), the evaluated dose and volume points were shown to be equivalent at a 95% confidence interval using the TOST-P procedure described in reference 27. All P values were below 5e-7.

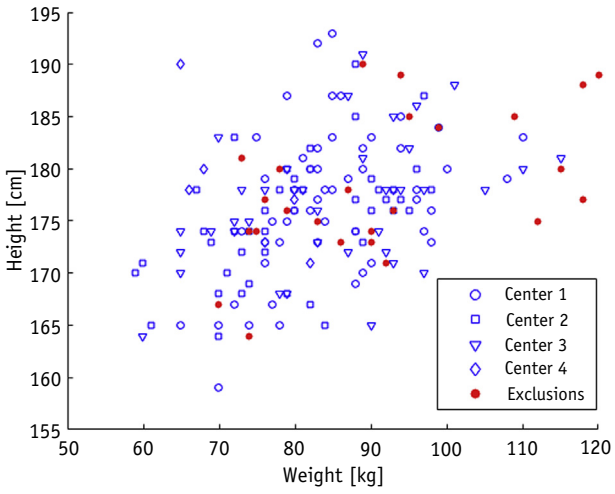

Fig. 1. Distribution of weight and height in the study population. Included patients, separated by included center, are presented in blue (circles, squares, triangles, and diamonds). Exclusions are presented in red (filled circles). (A color version of this figure is available at www.redjournal.org.)

The deviations between sCT and CT organ mean doses ranged between −1.15% and 1.42% (Fig. 2a-d). The 4 centers showed similar results. Small differences were seen between the prescriptions (ie, fractionation schemes found in Table 3), with an SD below 0.2% for the mean dose deviations.

The body-corrected sCTs showed smaller dose differences from the CT as compared with the original sCT for the 28 patients evaluated. The mean dose differences approached zero after correction. Standard deviations and maximum differences decreased (Figs. 3a and 3b). Gamma evaluation results are presented in Table 5 for the complete study population and the body-corrected subpopulation.

Discussion

The present study investigated the accuracy and robustness of a commercial software that enables the transition from a multimodal CT-MR workflow to an MRI-only workflow for external radiation therapy of prostate cancer. The MRI-only treatment planning procedure described in this study requires only minor changes in clinical routine, adding a large FOV T2-weighted MRI sequence of approximately 5 minutes and discarding the CT examination altogether.

The study was performed at 4 different clinics, with different clinical workflows, hardware, and software. Treatment plans generated using sCT were dosimetrically

Table 4 Mean dose deviation between sCT and CT

Parameter	Mean deviation sCT vs CT (% of prescribed dose or volume percentage difference) (1 SD)	Mean deviation sCT vs CT (absolute dose [Gy] or volume percentage point difference) (1 SD)
Body		
Maximum	0.18 (0.79)	0.13 (0.50)
PTV		
Mean	0.23 (0.42)	0.16 (0.28)
D99%	0.21 (0.50)	0.14 (0.35)
V95%	0.21 (0.65)	0.20 (0.62)
CTV		
Mean	0.24 (0.44)	0.17 (0.29)
Minimum	0.21 (0.54)	0.14 (0.36)
Bladder*		
Mean	0.04 (0.27)	0.03 (0.18)
Rectum		
Mean	0.16 (0.42)	0.10 (0.28)
V90%	1.37 (3.56)	0.18 (0.42)
V75%	0.21 (2.74)	0.03 (0.59)
V65%	0.26 (1.99)	0.04 (0.59)
Femoral heads†		
Mean	0.04 (0.18)	0.03 (0.11)
	0.05 (0.19)	0.03 (0.11)
Maximum	0.05 (0.38)	0.03 (0.26)
	0.07 (0.49)	0.06 (0.31)

Abbreviations: CT = computed tomography; CTV = clinical target volume; PTV = planning target volume; sCT = synthetic CT.

Total mean dose deviation between sCT and CT (145 patients). Deviations expressed in percentage of prescribed dose (mean, maximum, minimum, and D99%) or volume percentage difference (V95%, V90%, V75%, and V65%) (left column) and absolute change (in Gy) or volume percentage point difference (right column). Volume change evaluated for patients prescribed 78 Gy, according to the conventional arm of the HYPO-fractionated radiation therapy of intermediate-risk localized Prostate Cancer protocol.

* One patient excluded owing to structure missing in the clinical plan.

† Results for 105 patients, exclusions due to structure not contoured in clinical routine.

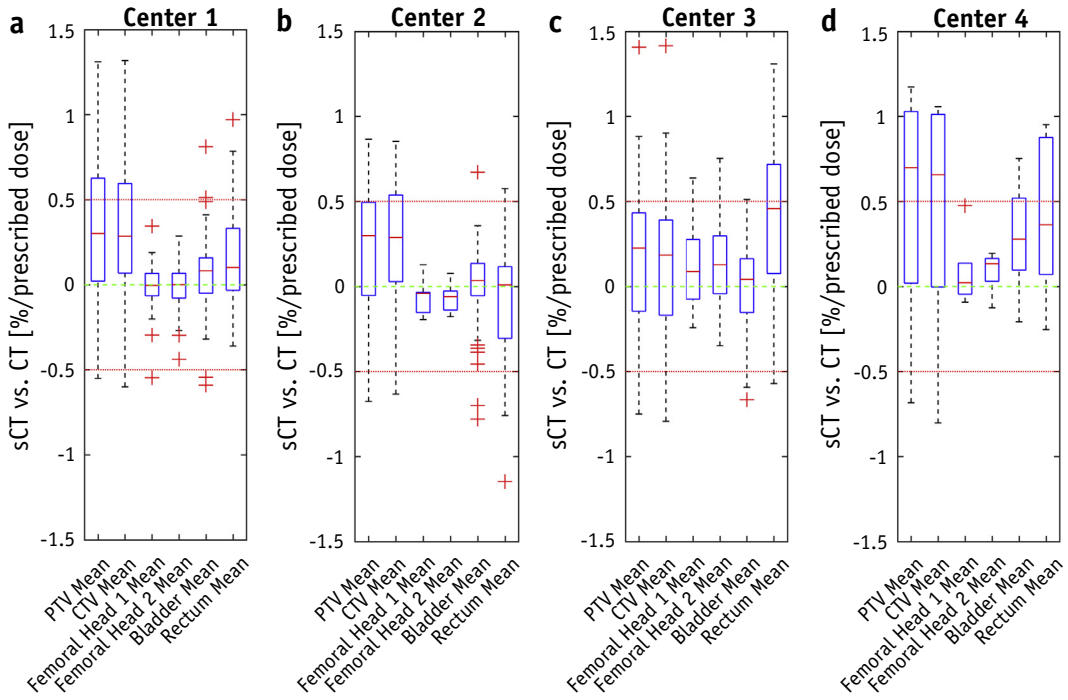

Fig. 2. (a-d) Individual center results. Deviations between synthetic computed tomography (sCT) and CT mean doses (sCT − CT, % of prescribed dose) at the 4 included centers for planning target volume (PTV), clinical target volume (CTV), femoral heads, bladder, and rectum.

accurate as compared with CT. In general, the dose differences observed between sCT- and CT-based plans were small and were shown to be statistically equivalent on a 95% confidence level within ±0.5%. The rectum volume criteria displays a higher mean deviation compared with the other OARs, which can be an influence of change in rectum filling or the replacement of gas with soft tissue in the sCT generation (21). A small systematic overshoot in Figure 2 is seen along with outliers near 1.5% dose deviation. The outliers were found to be patients with large outer body contour differences. The MR was frequently found systematically smaller in the anterior-posterior direction compared with the CT. This causes a higher sCT dose after recalculation. We hypothesize that this is an effect of the longer examination time of the MR compared with the CT. The study sequence was positioned at the end of the MR protocol for most patients, after an approximately 30- to 40-minute scan time. Patient relaxation could presumably cause the patients' anterior-posterior thickness to decrease and increase in the left-right direction, which was also seen in the data. In contrast to the MR examination, the CT examination is fast, and the patients are often more tense. The results indicate that the differences in patient external contour influence the dose comparison considerably, and after correcting for patient outline differences the differences are negligible. Hence, disparities in patient position are likely to be a major contributor in the small dose differences seen in our results. The differences in external patient contour also affected the gamma evaluation, but the results are still well within clinical acceptance criteria.

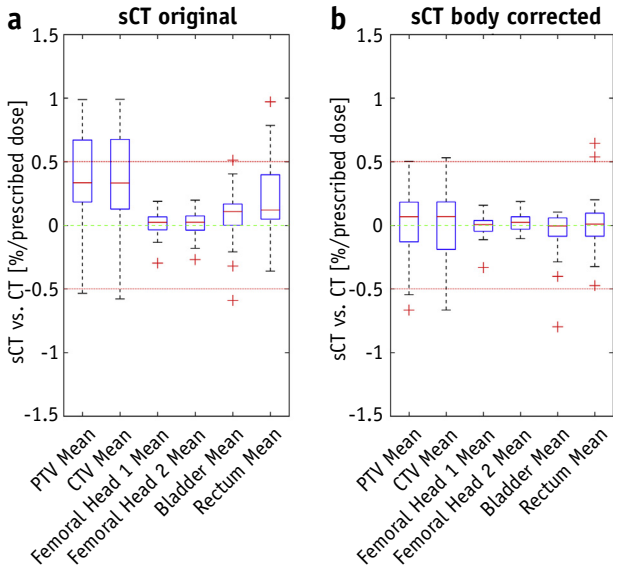

Fig. 3. (a, b) Body-corrected result. Results for 28 patients prescribed 78 Gy, evaluated with both an original synthetic computed tomography (sCT) and a body-corrected sCT compared with the CT. The original sCT/CT comparison (a) and the body-corrected sCT/CT comparison (b) for planning target volume (PTV), clinical target volume (CTV), femoral heads, bladder, and rectum mean doses (sCT − CT).

Previous studies on MRI-only prostate radiation therapy report results similar to ours. Commercially available MRCAT (MR for Calculating ATtenuation, Phillips

Table 5 Gamma evaluation

Parameter	3%/3 mm_g	2%/2 mm_g	1%/1 mm_g
Original sCT, complete study population (N = 145)			
PTV	99.99 (0.06)	99.97 (0.13)	98.28 (4.58)
Total	99.62 (0.36)	99.12 (0.63)	97.69 (1.26)
>15%	99.66 (0.42)	99.30 (0.68)	97.94 (1.35)
Subpopulation (n = 28), body-corrected sCT/original sCT			
PTV	100.00 (0.00)/100.00 (0.00)	99.98 (0.09)/100.00 (0.00)	99.64 (1.70)/97.82 (3.96)
Total	100.00 (0.00)/99.72 (0.28)	100.00 (0.01)/99.38 (0.38)	99.50 (0.45)/98.24 (0.79)
>15%	100.00 (0.00)/99.79 (0.29)	100.00 (0.01)/99.59 (0.42)	99.96 (0.14)/98.43 (0.98)

Abbreviations: PTV = planning target volume; sCT = synthetic computed tomography.
Values in parentheses are 1 SD.

Healthcare, Vantaa, Finland) was reported to produce treatment plans with dose differences CT-sCT of 0.25% (0.17% SD) to the planning target volume and 0.42% (0.50% SD) for organs at risk (28). In that study the entire study population (n = 13) was corrected for differences in patient external contour using an approach similar to the one presented in our study for the body-corrected subpopulation. A key difference between the method described in our study and MRCAT is that the latter is vendor specific. Other methods have been presented in the literature, also showing very high accuracy, but these are, to our knowledge, still in development or single-center use (12, 20, 29).

This study aimed at verifying the MRI-only method in a situation as close as possible to the clinical environment, without extensive corrections of the sCT data, to find the worst-case differences between the CT- and MR-based workflows. Because the MR and CT images were acquired at different occasions, ranging from 30 minutes to 1 day apart depending on the clinic, changes in internal anatomy were inevitable. The repositioning of the patient between modalities will also introduce differences in the external anatomy. Such differences could have been corrected for by using deformable registration, which is an approach that has been used previously (21). We opted to not employ such methods to preserve the integrity of the input data as much as possible. Therefore, the dose differences presented in our study are composed of actual errors in Hounsfield unit conversion as well as differences in patient anatomy and possible geometric distortions (remaining after correction) in the input MR data. Our study uses the conventional MR/CT workflow as a reference and recalculates the dose on the sCT for comparison. Another strategy would be to create a treatment plan optimized on the sCT for comparison against the CT, a method that has been shown to differ very little from our method (30, 31).

In this work the dosimetric accuracy in the MRI-only workflow is of primary interest. However, other important aspects of the treatment are also affected by removing the CT images, primarily patient positioning. Because many prostate cancer patients are positioned using implanted gold fiducials, configuration of suitable marker localization sequences that can be acquired in immediate succession to the sequence used for sCT generation is important. To achieve a workflow with improved geometric accuracy compared with the CT/MR workflow, the uncertainty in the fiducial marker localization cannot exceed the MR-CT registration uncertainty. A future improvement would be to develop markers that are visible directly on the treatment planning sequence. Further, it would be of importance to the MRI-only workflow to integrate automatic fiducial detection (32). If markers are not used, the sCT should work well for matching against cone-beam CT scans and orthogonal X rays or megavoltage portal images, earlier demonstrated (33). The geometric fidelity of the sCT images will be investigated for such purpose in a future study.

In the implementation of MRI-only, it becomes crucial to ensure properly executed MRI procedures. Exclusions in this study were mainly due to improper inclusion or operator fault, which could be captured at an early stage with proper MR quality assurance (QA) procedures and staff training. Eight patients had insufficient target coverage in the slice direction. This was a consequence of the study design. The extra acquisition time allowed for adding on the sCT sequence to the protocol was restricted to approximately 5 minutes. In this time frame the necessary number of slices to cover the entire target volume for the 8 patients could not be acquired. This specific issue will not be the case in an actual MRI-only environment, with a dedicated MRI-only protocol. Education and training are important parts of the implementation process of MRI-only and are necessary to avoid operator fault at the MR scanner. Mistakes, such as an inadvertently turned-off 3-dimensional correction, could be prevented by staff training and working documents. Automatic control of the MR parameters at the MR scanner could be a possible method to detect erroneous parameter settings. This would not prevent operator faults, although it would be detected at an early stage of the process. Although no serious errors in sCT generation could be found in this study, a routine to detect potential errors is still needed. A simple sanity check of the Hounsfield unit distribution would probably be sufficient, or the use of patient-specific QA if a higher level of certainty is desirable. Methods for such QA procedures are an important part of MRI-only and should be developed and tested thoroughly before an implementation of the technique can be considered completed.

When the registration step between the treatment planning CT and MR images is eliminated, an important uncertainty is removed. The small differences found between CT- and sCT-based dose calculations in the present study must be set in contrast to the total uncertainty in radiation therapy. When considering the complete workflow, including uncertainties in beam calibration, relative dosimetry, dose calculations, and dose delivery, the International Commission on Radiation Protection states an estimated standard uncertainty of 5% in a clinical setup (34). The added uncertainty of a synthetically generated dose calculation image, shown in our study to differ only by fractions of a percent from CT-based dose calculations, is likely negligible in comparison to the total uncertainty. The dose differences presented in our study are well within previously published criterion of reliable MRI-only dose calculations (31). Furthermore, most of the dose difference is likely to stem from the difficulty in comparing images acquired at different occasions and not from the actual sCT conversion in itself, analogous to comparing fractional doses on cone-beam CTs in the traditional workflow.

Conclusions

In conclusion, the MR-OPERA study shows that an MRI-only treatment planning workflow using MriPlanner software is dosimetrically accurate and robust for a variety of vendors, field strengths, and treatment techniques. The differences observed between CT and sCT dose distribution are small, and when compared with other uncertainties in radiation therapy they are negligible. The suggested method will allow implementation of an MRI-only workflow for external prostate radiation therapy in most clinics.

References

1. Karlsson M, Karlsson MG, Nyholm T, Amies C, Zackrisson B. Dedicated magnetic resonance imaging in the radiotherapy clinic. *Int J Radiat Oncol Biol Phys* 2009;74:644-651.
2. Datta NR, David R, Gupta RK, et al. Implications of contrast-enhanced CT-based and MRI-based target volume delineations in radiotherapy treatment planning for brain tumors. *J Cancer Res Ther* 2008;4:9-13.
3. Prabhakar R, Haresh KP, Ganesh T, et al. Comparison of computed tomography and magnetic resonance based target volume in brain tumors. *J Cancer Res Ther* 2007;3:121-123.
4. Rasch CR, Steenbakkers RJ, Fitton I, et al. Decreased 3D observer variation with matched CT-MRI, for target delineation in nasopharynx cancer. *Radiat Oncol* 2010;5:21.
5. Khoo EL, Schick K, Plank AW, et al. Prostate contouring variation: Can it be fixed? *Int J Radiat Oncol Biol Phys* 2012;82:1923-1929.
6. Roach M 3rd, Faillace-Akazawa P, Malfatti C, et al. Prostate volumes defined by magnetic resonance imaging and computerized tomographic scans for three-dimensional conformal radiotherapy. *Int J Radiat Oncol Biol Phys* 1996;35:1011-1018.
7. Nyholm T, Nyberg M, Karlsson MG, Karlsson M. Systematisation of spatial uncertainties for comparison between a MR and a CT-based radiotherapy workflow for prostate treatments. *Radiation oncology* 2009;4:54.
8. van Herk M, Remeijer P, Rasch C, et al. The probability of correct target dosage: Dose-population histograms for deriving treatment margins in radiotherapy. *Int J Radiat Oncol Biol Phys* 2000;47:1121-1135.
9. Hsu SH, Cao Y, Huang K, et al. Investigation of a method for generating synthetic CT models from MRI scans of the head and neck for radiation therapy. *Phys Med Biol* 2013;58:8419-8435.
10. Johansson A, Karlsson M, Nyholm T. CT substitute derived from MRI sequences with ultrashort echo time. *Medical physics* 2011;38:2708-2714.
11. Paradis E, Cao Y, Lawrence TS, et al. Assessing the dosimetric accuracy of magnetic resonance-generated synthetic CT images for focal brain VMAT radiation therapy. *Int J Radiat Oncol Biol Phys* 2015;93:1154-1161.
12. Dowling JA, Lambert J, Parker J, et al. An atlas-based electron density mapping method for magnetic resonance imaging (MRI)-alone treatment planning and adaptive MRI-based prostate radiation therapy. *Int J Radiat Oncol Biol Phys* 2012;83:e5-e11.
13. Greer PB, Dowling JA, Lambert JA, et al. A magnetic resonance imaging-based workflow for planning radiation therapy for prostate cancer. *Med J Aust* 2011;194:S24-S27.
14. Sjolund J, Forsberg D, Andersson M, et al. Generating patient specific pseudo-CT of the head from MR using atlas-based regression. *Phys Med Biol* 2015;60:825-839.
15. Stanescu T, Jans HS, Pervez N, et al. A study on the magnetic resonance imaging (MRI)-based radiation treatment planning of intracranial lesions. *Phys Med Biol* 2008;53:3579-3593.
16. Andreasen D, Van Leemput K, Edmund JM. A patch-based pseudo-CT approach for MRI-only radiotherapy in the pelvis. *Med Phys* 2016;43:4742.
17. Jonsson JH, Karlsson MG, Karlsson M, Nyholm T. Treatment planning using MRI data: an analysis of the dose calculation accuracy for different treatment regions. *Radiation oncology* 2010;5:62.
18. Korhonen J, Kapanen M, Keyrilainen J, et al. Absorbed doses behind bones with MR image-based dose calculations for radiotherapy treatment planning. *Med Phys* 2013;40:011701.
19. Lambert J, Greer PB, Menk F, et al. MRI-guided prostate radiation therapy planning: Investigation of dosimetric accuracy of MRI-based dose planning. *Radiother Oncol* 2011;98:330-334.
20. Kim J, Glide-Hurst C, Doemer A, et al. Implementation of a novel algorithm for generating synthetic CT images from magnetic resonance imaging data sets for prostate cancer radiation therapy. *Int J Radiat Oncol Biol Phys* 2015;91:39-47.
21. Siversson C, Nordstrom F, Nilsson T, Nyholm T, Jonsson J, Gunnlaugsson A, et al. Technical Note: MRI only prostate radiotherapy planning using the statistical decomposition algorithm. *Medical physics* 2015;42:6090-6097.
22. Deasy JO, Blanco AI, Clark VH. CERR: A computational environment for radiotherapy research. *Med Phys* 2003;30:979-985.
23. Widmark A. Phase III study of HYPOfractionated RadioTherapy of intermediate risk localised Prostate Cancer. Available at: www.isrctn.com/ISRCTN45905321. Accessed May 1, 2017.
24. Low DA, Harms WB, Mutic S, et al. A technique for the quantitative evaluation of dose distributions. *Med Phys* 1998;25:656-661.
25. Nyholm T, Berglund M, Brynolfsson P, Jonsson J. EP-1533: ICE-Studio- An interactive visual reaserch tool for image analysis. *Radiotherapy and Oncology* 2015;115.
26. Wendling M, Zijp LJ, McDermott LN, et al. A fast algorithm for gamma evaluation in 3D. *Med Phys* 2007;34:1647-1654.
27. Mara CA, Cribbie RA. Paired-samples test of equivalence. *Commun Stat Simul Comput* 2012;41:15.
28. Köhler M, Vaara T, Grootel MV, et al. MR-only simulation for radiotherapy planning. Amsterdam, The Netherlands: Philips white paper; 2015.
29. Korhonen J, Kapanen M, Keyrilainen J, et al. A dual model HU conversion from MRI intensity values within and outside of bone segment for MRI-based radiotherapy treatment planning of prostate cancer. *Med Phys* 2014;41:011704.
30. Jonsson JH, Akhtari MM, Karlsson MG, Johansson A, Asklund T, Nyholm T. Accuracy of inverse treatment planning on substitute CT

images derived from MR data for brain lesions. *Radiat Oncol* 2015; 10:13.
31. Korsholm ME, Waring LW, Edmund JM. A criterion for the reliable use of MRI-only radiotherapy. *Radiat Oncol* 2014;9:16.
32. Ghose S, Mitra J, Rivest-Henault D, et al. MRI-alone radiation therapy planning for prostate cancer: Automatic fiducial marker detection. *Med Phys* 2016;43:2218.
33. Korhonen J, Kapanen M, Sonke JJ, et al. Feasibility of MRI-based reference images for image-guided radiotherapy of the pelvis with either cone-beam computed tomography or planar localization images. *Acta Oncol* 2015;54:889-895.
34. International Commission on Radiation Protection. Prevention of accidents to patients undergoing radiation therapy. ICRP publication 86. *Ann ICRP* 2000;30.